3D Survey with Apple LiDAR Sensor—Test and Assessment for Architectural and Cultural Heritage

Giuseppina Vacca

Department of Civil and Environmental Engineering and Architecture, University of Cagliari, 09123 Cagliari, Italy; vaccag@unica.it

Abstract: The documentation and metric knowledge of architectural and cultural heritage is becoming an increasingly important need, especially concerning the state of degradation of some historical assets and the associated required interventions. In this context, the metric documentation of the investigated heritage becomes fundamental for a complete knowledge of the asset in order to support architects and engineers in the restoration process. Recently, methods and geomatic instrumentation have been developed for the survey of cultural heritage aiming at optimizing costs and time. Apple has integrated into its devices a LiDAR sensor capable of providing a 3D model of spaces and objects. The present paper aims to investigate the potential of this sensor for the production of 3D models of cultural heritage assets in terms of accuracy and applicability. Consistently, four apps developed for the generation of point clouds for five case studies related to architectural-cultural heritage assets have been tested. We used Polycam, Sitescape, 3D Scanner and Scaninverse. The results obtained allow us to conclude that the Apple LiDAR sensor can be used for the creation of 3D models for applications and metric documentation of architectural and cultural heritage that are not particularly complex in form and texture.

Keywords: iPad Pro; low-cost LiDAR sensor; 3D model; cultural heritage

1. Introduction

The documentation and metric knowledge of cultural heritage is becoming crucial if we consider the state of degradation of the majority of historical built heritage and the associated restoration interventions. For these valuable architectures, in-depth metric documentation is fundamental for an overall understanding of these structures, and, in turn, to support architects and engineers in optimizing restoration, conservation, safeguarding and artifact enhancement [1–4]. Recently, however, public funding intended for geometric investigations has been reduced, leading stakeholders and researchers to develop low-cost geomatic tools and methodologies to tackle this necessity, without compromising the metric accuracy too much [5]. In this respect, among the low-cost geomatic techniques, multi-image photogrammetry [6–9] is certainly the most effective in facilitating the democratization of the metric documentary process and, thus, in contributing to a wider involvement of users without any specific geomatics expertise.

Via multi-image photogrammetry, it is possible to obtain complete and exhaustive 3D metric surveys with a rapid and intuitive approach [10,11]. Several examples of this are reported in the literature: ranging from architectural applications [12–14] to the control and monitoring of structures [15,16], or to environmental and forestry assessments [17–19]. In particular, Structure-from-Motion (SfM) algorithms, used in multi-image photogrammetry, produce accurate point clouds with good repeatability [20] and are well suited for the production of metric documentation.

For 3D metric surveys, new miniaturized and low-cost sensors have recently paved the way for the cost-effective survey and 3D modeling of buildings or historical–cultural heritage assets. Among these tools, the laser scanning sensor implemented since 2020 in

Apple's iPhone (from 12 Pro) and iPad Pro is worth mentioning. The complete technical specifications of this sensor—recommended mostly for Augmented Reality (AR) and Virtual Reality (VR)—are not available, but, from the scientific literature, it seems that it consists of a solid-state LiDAR (SSL), i.e., a type of LiDAR which, unlike traditional sensors, does not use motorized mechanical parts (ensuring greater reliability) [21–23]. The SSL sensor is based on a silicon chip characterized by a longer operating life and smaller dimensions compared to traditional LiDARs [24]. Some authors [20,25] claim that the LiDAR present in Apple devices uses an emitter composed of a vertical-cavity surface-emitting laser (VCSEL) producing laser pulses by using a Diffraction Optics Element (DOE) and a Single-Photon Avalanche Diode (SPAD) receiver. The LiDAR sensor is classified as a dToF (direct Time-of-Flight) device directly measuring the time between the emission of light and its reception [26]. The points measured by the LiDAR sensor are combined with the information provided by the RGB camera present in the device and the range declared by Apple is 5 m. Furthermore, from various studies, it seems that there are no differences between the LiDAR sensors mounted on the iPhone and the iPad [27].

The use of the Apple LiDAR sensor is possible only through the dedicated apps that can be downloaded from the App Store. Their combined use allows, in addition to the acquisition of the points, the exporting of the point cloud and the mesh in various formats. For all apps, it exists as both a free-of-charge version, which makes it possible to export merely the mesh and/or point cloud, and as a paid version (with a monthly or yearly fee) with more advanced functions targeting mainly metric documentation.

Since the advent of the LiDAR sensor in Apple devices, several apps have been developed and research has been carried out by research groups to study the geomatic potential and functions of both the sensor and the dedicated apps.

In [28], researchers demonstrate the potential and functionality of both sensors in the iPhone and iPad and of some iOS applications (SiteScape, 3DScanner App and EveryPoint). Accuracies are investigated in different relevant scenarios, such as indoor and outdoor, static or dynamic configuration, and in different types of cultural and architectural heritage (e.g., statues, decorated rooms and external facades). In addition, concerning heritage documentation, Murtiyos et al. [20] studied the potential of the sensor with respect to multi-image photogrammetry and Terrestrial Laser Scanning of a small object, a facade and a 3D space, using two apps: Every Point and SiteScape. By contrast, in [29], some geometric aspects of the surveys with the Apple sensor have been addressed: local precision, global correctness and surface coverage for indoor and outdoor environments.

The Apple LiDAR sensor has been also used and tested for non-architectural metric surveys: one of the main studies concerns its use for measuring the metric parameters of trees. In this respect, in [25], it was used to study and provide forest inventory variables, validating the results by comparing them with Personal Laser Scanning (PLS) techniques.

The purpose of the present paper is to contribute towards painting a complete picture of the potential of the LiDAR sensor incorporated in the third generation iPad Pro [30] with respect to its effectiveness in both architectural applications (i.e., reconstructions of architectural elements, facades or decorative elements) and assessments of cultural heritage assets (e.g., ancient musical instruments). Consistently, we tested the LiDAR sensor for the survey of elements with different shapes and textures, using four different apps (among the most used on the market): PolyCam [31], SiteScape [32], 3DScanner [33] and Scaninverse [34]. The results obtained using the LiDAR sensor were validated using data from a Terrestrial Laser Scanner.

2. Materials and Methods

The research presented in the paper is part of the research on the study of the potential and functionality of the LiDAR sensor present in the Apple iPad Pro (3rd generation) and of some apps developed for 3D surveying. The iPad Pro has the following specifications: 11″ Liquid Retina display, weight of 468 g, 512 GB of memory, 8-core CPU, 8 GB RAM and iOS

15.0.2 software version. It is equipped with a 12 MP wide-angle and 10 MP ultra-wide-angle RGB camera system and a LiDAR sensor [30].

Four different scanning apps were used and tested: Polycam, Sitescape, 3D Scanner App and Scaninverse. All four apps can be used in free mode or through a paid license (Polycam and SiteScape). Of the four apps, only the monthly license for Polycam was purchased, at a cost of $6.99/month, allowing us to export the point clouds in different formats (a possibility prevented in the free version, which is capable of exporting only the mesh in glTF format). Table 1 shows the main features of the four apps.

Table 1. Features of the four apps used.

Name	License	Price	Point Cloud	Mesh	File Formats	Version
Polycam	Free/By charge	6.99 $/month	Yes	Yes	.ply, .las and others	2.3.9
SiteScape	Free/By charge	49.99 $/month	Yes	Yes	.ply E57 and others	1.6.8
3D Scanner App	Free		Yes	Yes	xyz; ply; pts; las; and others	2.0.8
Scaninverse	Free		Yes	Yes	.ply, .las and others	2.0.3

These apps allow the user to set different parameters before acquiring and/or processing the point cloud. Below, a description of the used apps and the associated parameters is discussed. Figure 1 shows screenshots of the four investigated apps.

(A) (B)

(C) (D)
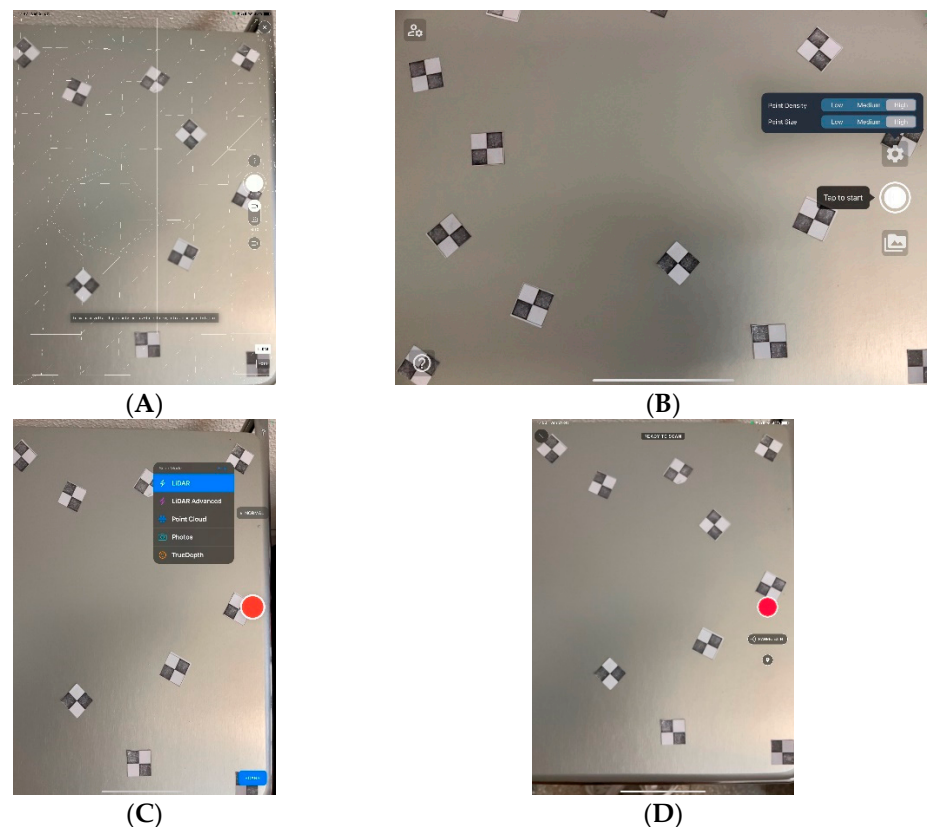
Figure 1. Used apps: (**A**) Polycam; (**B**) Sitescape; (**C**) 3D Scanner; (**D**) Scaninverse.

Polycam (version 2.3.9 by charge—Figure 1A) allows the user to scan objects by choosing between the LiDAR and ROOM options. This last option allows obtaining, in addition to the point cloud of the scanned room, the planimetry in dxf format. In the point cloud processing phase, it is possible to choose between Fast (allowing for fast processing for acquisition verification), Space (designed for space scans), Object (for object scans) and Custom modes. For the Custom mode, it is possible to choose the Depth Range (from 0.1 to 6 m), the Voxel Size (from 3 mm to 27 mm) and the simplification to be applied to the mesh (in percentage).

SiteScape (Version 1.6.8 free—Figure 1B) allows for customization of the "point density" ("low", "medium" or "high") and "point size" ("low", "medium" or "high). The "point density" defines the acquired number of points, where the "medium"/"high" quality corresponds, respectively, to two/four times the number of points obtained in the "low" quality mode. Finally, the "point size" influences only the dimensions of points visible in real-time, not the acquired data set itself [11].

3D Scanner App (version 2.0.8 free—Figure 1C) provides two scanning modes, named "LiDAR" and "LiDAR Advanced". The "LiDAR" has no parameters to set; it provides the simplest mode to capture a 3D scene. In the processing phase, there is the possibility to choose between the HD, Medium, Fast and Custom options, where varying some parameters is possible. This mode is recommended for measuring large spaces. The "LiDAR Advanced" option allows the operator to produce a better scan, offering four different settings: "max depth" (ranging between 0.3 m and 5.0 m with a step of 0.1 m), "resolution" (ranging from 5 mm to 50 mm with a step of 1 mm), "confidence" ("low", "medium" or "high") and "masking" ("none", "object" or "person").

Scaninverse (v2.0.1 free—Figure 1D) allows the user to select the type of object to scan between small object, medium object and large object/area, based on its size. During processing, the user can opt for the Speed mode (10 mm resolution), the Area mode (5 mm resolution, which is suitable for rooms and spaces) and the Detail mode (for textured objects).

To evaluate the Apple LiDAR sensor's potentiality and that of the 4 apps chosen, different types of objects were chosen; in particular, the range declared by Apple being 5 m, elements belonging to assets of the architectural-cultural heritage were chosen. In particular, tests were carried out on vaults and columns of buildings, on facades and on objects such as a small stone fountain and a wooden violin.

In Figures 2–6, the different case studies are shown.

Figure 2. Vault of the Santa Maria del Monte Church.

Figure 3. Column in the Department of Architecture.

Figure 4. Facade.

Figure 5. Stone fountain.

Figure 6. Violin.

In order to evaluate the accuracy of the scans performed using the LiDAR sensor, all the case studies were also surveyed with two Terrestrial Laser Scanners: the Faro Focus 3D and the Leica HDS 7000.

The Faro Focus 3D Terrestrial Laser Scanner is a compact scanner characterized by an operative range spanning 0.6 to 120 m, with a ranging error of $\pm$2 mm for scanner–object distances between 10 and 25 m.

The HDS7000 Laser scanner is a scanner characterized by an operative range between 0.3 m and 187 m, with a ranging error of $\pm$ 1 mm for scanner–object distances between 10 and 25 m.

The scans were processed using the JRC Reconstructor software v. 3.1.0 by Gexcel Ltd., Hong Kong, China [35]. All clouds from the apps were aligned to those from the TLS by using the JRC Reconstructor software.

The validation of the point clouds of the LiDAR sensor was performed by means of the CloudCompare software [36] and, specifically, the Cloud-to-Cloud Distance (C2C) tool. Cloud-to-cloud (C2C) analysis calculates the minimal distance between every point of the models using the nearest neighbor algorithm. Furthermore, the software allows the evaluation of statistical parameters, such as the minimal distance, maximal distance, average distance and standard deviation.

3. Results

The following paragraphs present the results obtained using the LiDAR sensor incorporated into the iPad Pro when tested during the five investigated cases. For each case study, the following parameters were evaluated:

- Number of points detected by each scan for the same element portion;
- Scanning times;
- Statistical values of the C2C comparison between the scan with the LiDAR sensor and the TLSs (Faro Focus 3D or HDS7000).

3.1. Case 1: Vault of the Santa Maria del Monte Church (Cagliari)

The first case study concerns the survey of one of the vaults in the Church of Santa Maria del Monte located in the city of Cagliari (Italy). It is a cross vault inside the church built, in Catalan Gothic style, in the 16th century [36].

Taking into account that the maximum range of the LiDAR sensor is 5 m, the survey was performed on a gallery, which overlooks the vault, and from a distance of about 5 m. Data from the vault were collected by using all four apps. In the following, the parameters used for scanning and processing are presented for all four apps:

Polycam: the scan was processed in the "Space" mode;

Sitescape: "Point Density" and "Point Size" were set to "High";

3D Scanner: the scan was performed in "LiDAR Advanced" mode, choosing (i) "Max Depth" equal to 5 m, (ii) "resolution" equal to 5 mm, (iii) "Confidence" equal to "High", and iv) "Masking" equal to "Object";

Scaninverse: the scan was performed in "Large object" mode and the processing in "Region" mode.

For validation purposes, the vault was also measured using the TLS HDS7000 without the external digital camera; therefore, the point cloud is represented only with its reflectance. The scan was performed from the balcony in "High" mode with a resolution of 6.3 mm/10 m. Capture times were relatively short (about 5 min) for each of the apps and the TLS.

Table 2 shows the number of points in the vault point cloud (corresponding to the same vault portion; see Figure 7).

Table 2. Number of points of the point clouds for the vault.

Dataset	N° of Points
HDS	20,686.478
Polycam	2353.90
Sitescape	8774.849
3D Scanner App	3198.208
Scaninverse	245.556

(**A**)

(**B**)

(**C**)

Figure 7. *Cont.*

(D) (E)
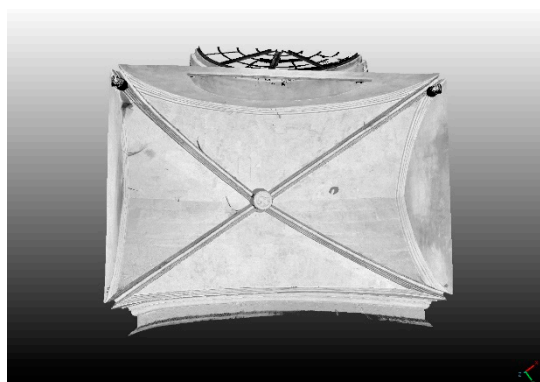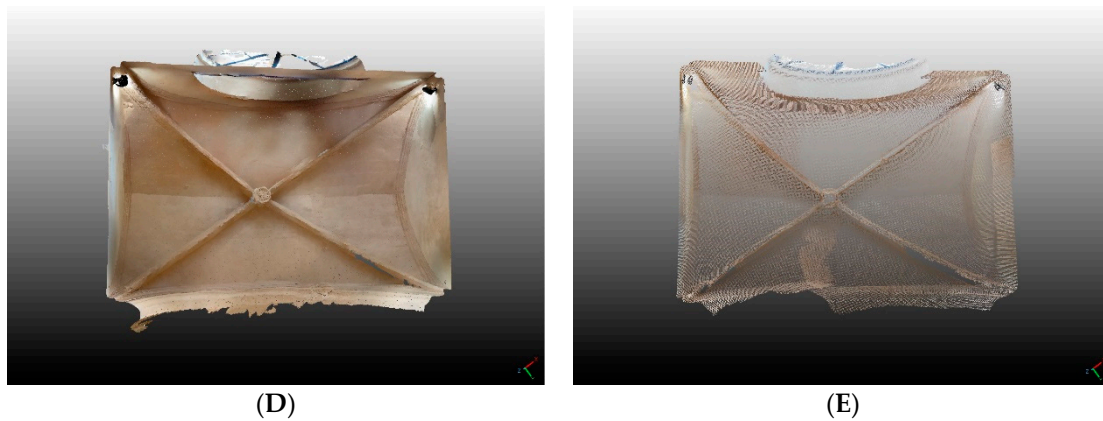
Figure 7. Point clouds of the vault: (**A**) HDS7000; (**B**) Polycam; (**C**) Sitescape; (**D**) 3D Scanner; (**E**) Scaninverse.

From the analysis in Table 2 and from the images of the point clouds (Figure 7), their different resolutions are immediately evident, and, in particular, the point cloud obtained with Scaninverse (Figure 7E) appears to be the one with the worst resolution, although the app was still able to effectively reconstruct the main features of the vault. To evaluate the accuracy of the point clouds, they were compared against the one provided by the TLS, via the Cloud-to-cloud (C2C) analysis. Table 3 shows the statistical parameters associated with these comparisons, whereas Table 4 presents the percentages of points falling into the different ranges. This kind of preliminary analysis was useful to set a threshold to exclude possible outliers. In the case of the vault, the threshold was chosen equal to 10 cm. For Polycam, 2% of the points exceeded this threshold; for Sitescape, 10%; for 3D Scanner, 1%; and for Scaninverse, 14%.

Table 3. C2C analysis—statistical parameters of the comparisons between the TLS and the apps' point clouds.

App	Polycam	SiteScape	3D Scanner	Scaninverse
Min (m)	0	0	0	0
Max (m)	0.239	0.412	0.215	0.227
Mean (m)	0.014	0.032	0.018	0.034
Dev. Stand (m)	0.030	0.042	0.032	0.040

Table 4. C2C analysis—percentages of points in the different distance ranges.

App	Polycam	SiteScape	3D Scanner	Scaninverse
<1 cm	26%	11%	25%	12%
1 cm–3 cm	40%	25%	34%	25%
3 cm–5 cm	25%	27%	24%	16%
5 cm–10 cm	7%	27%	16%	33%
>10 cm	2%	10%	1%	14%

From Tables 3 and 4 and Figures 8–11 (showing the discrepancy maps), the best results are clearly obtained using Polycam and 3D Scanner, which are characterized by maximum discrepancies around 20 cm, with an average mismatch of about 1.5 cm and a standard deviation of about 3 cm. Table 4 demonstrates that Polycam has the highest percentage (66%) of points falling in the first two ranges (between 0 cm and 3 cm) and 3D Scanner provides results with 59% in the smallest ranges, whereas the other two apps have much lower percentages.
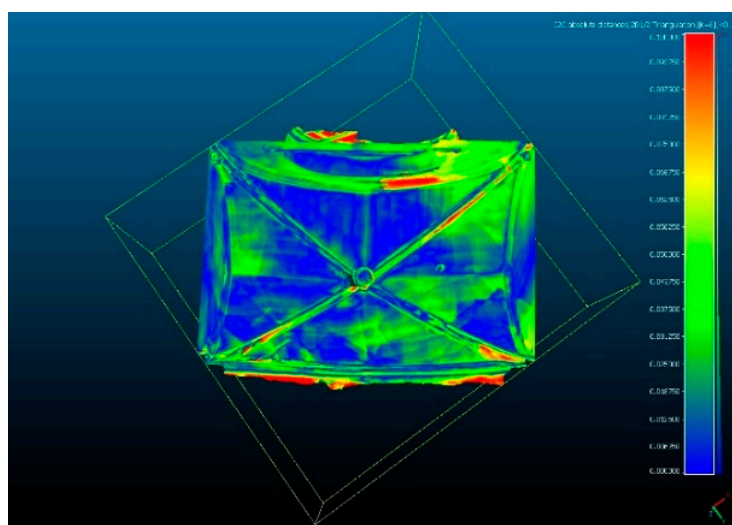
Figure 8. Discrepancy (m) map between TLS' and Polycam's point clouds.
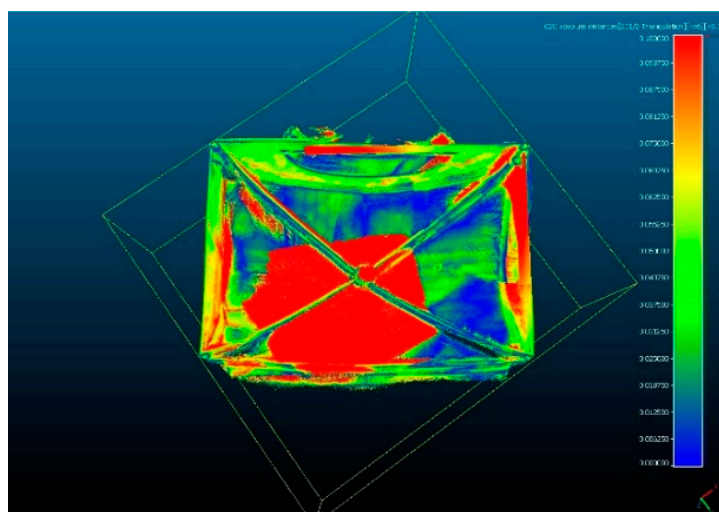
Figure 9. Discrepancy (m) map between TLS' and Sitescape's point clouds.
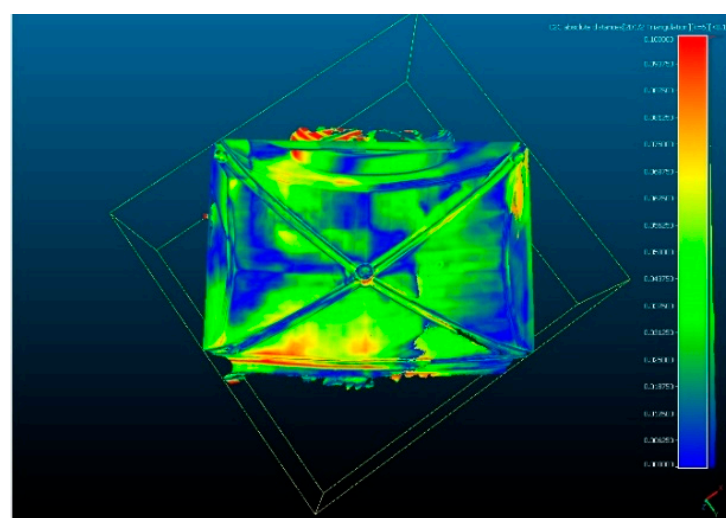
Figure 10. Discrepancy (m) map between TLS' and 3D Scanner's point clouds.
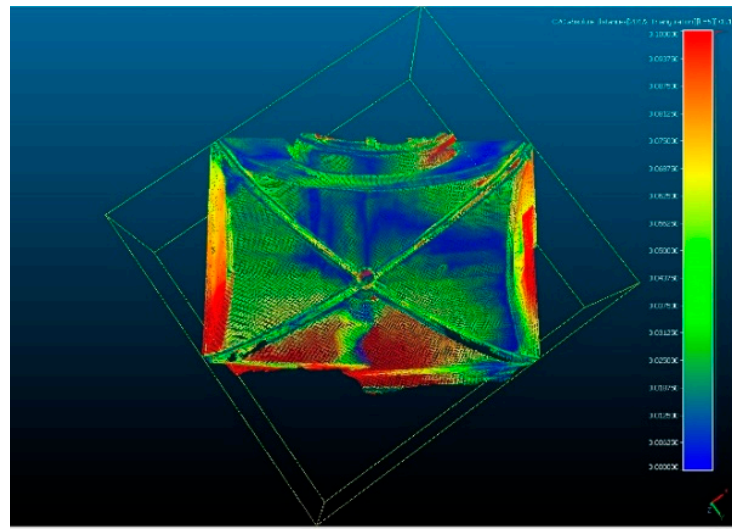
Figure 11. Discrepancy (m) map between TLS' and Scaninverse's point clouds.

3.2. Case 2: Column

The second case relates to a survey of a column located inside the cloister of the Architecture Building of the University of Cagliari. The column height is 4.60 m.

The acquisition with the LiDAR sensor was performed by rotating around the column from the bottom to the top. The scan parameters used for the different apps were the same as those selected for Case 1 (Section 3.1). It should be noted that all apps faced difficulties while acquiring data in the upper part of the column. Therefore, to obtain satisfactory results, the survey had to be repeated several times.

For the point cloud validation, the column was also measured using the TLS Faro Focus 3D. The scans were made at $\frac{1}{4}$ resolution, $3\times$ quality (7 mm/10 m resolution) and with an overlap between scans of at least 30%. With these parameters, four scans were performed from different station points in order to obtain a complete scan of the column.

The acquisition times were relatively short for the 4 apps: about 5 min for each app. By contrast, for the TLS, 4 color scans were acquired and each took 6 min, on top of which the data processing time (performed using the JRC Reconstructor software version 3.1.0 by Gexcel Ltd.) needs to be added.

Table 5 shows the number of points in the point cloud (relative to the same portion of the column; Figure 12).

Table 5. Number of points in the point clouds for the column.

Dataset	N° of Points
Focus 3D	804.275
Polycam	386.238
Sitescape	7322.792
3D Scanner App	108.361
Scaninverse	1094.006
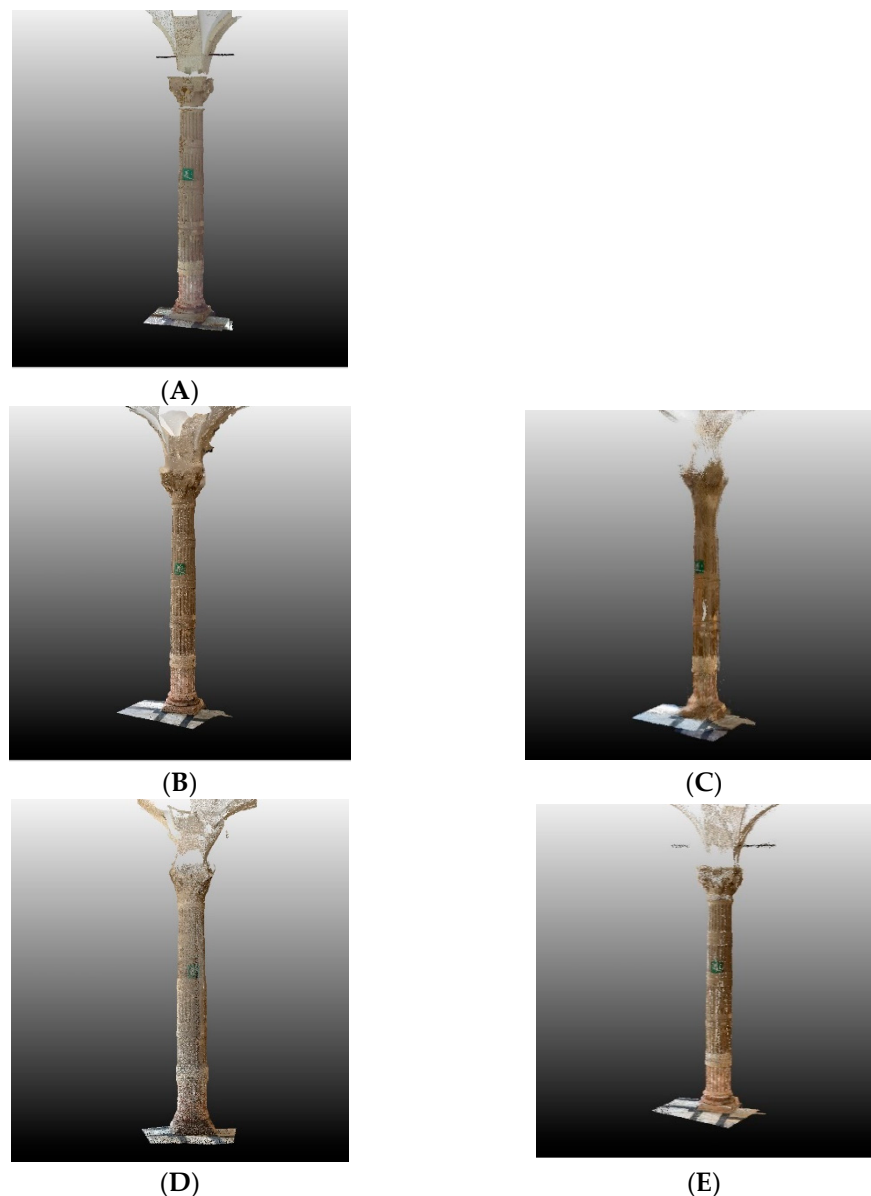
Figure 12. Point clouds of the column: (**A**) Focus 3D; (**B**) Polycam; (**C**) Sitescape; (**D**) 3D Scanner; (**E**) Scaninverse.

From the analysis of Table 5, and from the images of the point clouds (Figure 12), the different resolutions are immediately evident and, in particular: (i) the point cloud obtained with the 3D Scanner App (Figure 12D) appears to provide the poorest reconstruction; (ii) Sitescape (Figure 12C)—despite having the largest number of points—had difficulties in properly reconstructing the 3D model of the target (the column seems twisted). As before, to quantitatively assess the accuracy of the point clouds from the different apps, they were compared against the TLS measurements by means of a Cloud-to-Cloud (C2C) analysis. The results are shown in Table 6. Table 7 shows the percentages of points falling into different mismatch ranges. Analogously to Case 1, a threshold was set to prevent biases from probable outliers. Consistently, the same threshold value as before (10 cm) was set: (i) 8% of the detected points exceeded this threshold for Polycam; (ii) 4% for Sitescape; (iii) 10% for 3D Scanner; and (iv) 0.4% for Scaninverse.

Table 6. Statistical parameters of the comparisons between the TLS data and the apps' point clouds.

App	Polycam	SiteScape	3D Scanner	Scaninverse
Min (m)	0	0	0	0
Max (m)	0.474	0.498	0.534	0.791
Mean (m)	0.025	0.030	0.037	0.008
Dev. Stand (m)	0.060	0.037	0.026	0.026

Table 7. C2C analysis—percentages of points in the different distance ranges.

App	Polycam	SiteScape	3D Scanner	Scaninverse
<1 cm	52%	19%	22%	59%
1 cm–3 cm	26%	29%	48%	35%
3 cm–5 cm	7%	25%	13%	5%
5 cm–10 cm	7%	23%	7%	0.6%
>10 cm	8%	4%	10%	0.4%

From Tables 6 and 7, and Figures 13–16 (the discrepancy map for the column's case), it is clear that all apps—except, again, SiteScape—provide satisfactory results. Scaninverse shows the best performances, with 94% of points having a mismatch with respect to the TLS point cloud between 0 and 3 cm. In terms of accuracy, Scaninverse is followed by Polycam (with 78%) and 3D Scanner (with 70%).
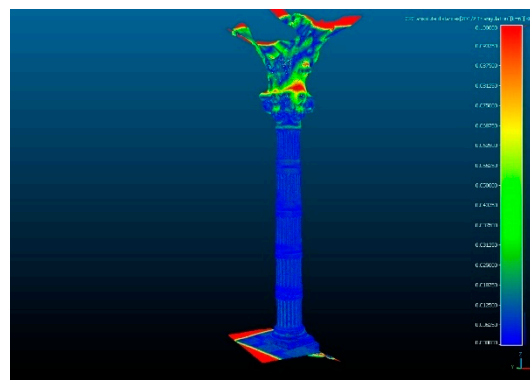
Figure 13. Discrepancy (m) map between TLS' and Polycam's point clouds.
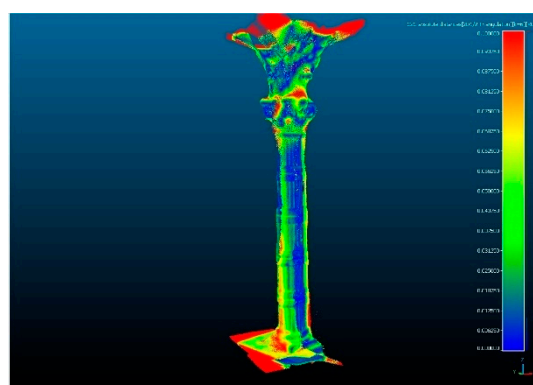
Figure 14. Discrepancy (m) map between TLS' and Sitescape's point cloud.
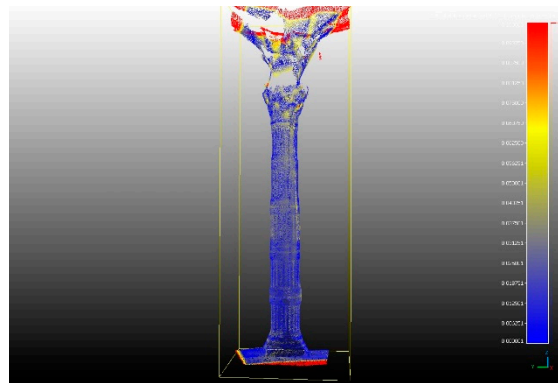
Figure 15. Discrepancy (m) map between TLS' and 3D Scanner's point clouds.
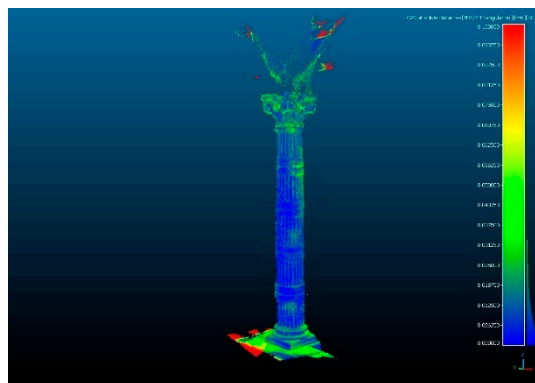
Figure 16. Discrepancy (m) map between TLS' and Scaninverse's point clouds.

To better examine the point clouds obtained from the four apps, four horizontal sections, at specific heights, were also analyzed (Figure 17) and compared with similar sections extracted from the TLS point cloud. The sections were extracted using the Cloud Compare software.
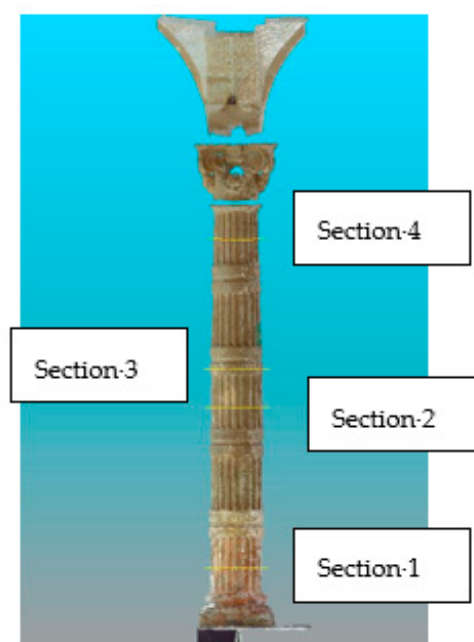
Figure 17. Column sections.

Figures 18–21 present the four sections as obtained, respectively, from the apps and the TLS: (i) the TLS section is shown in black; (ii) the Polycam section in blue; (iii) the Sitescape section in orange; (iv) the 3D Scanner section in pink; and (v) the Scaninverse section in green.
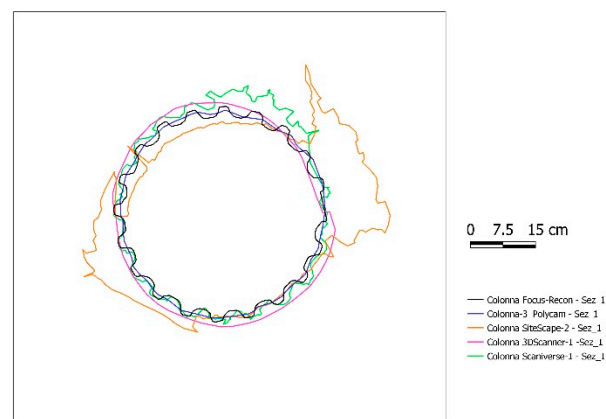
Figure 18. Section 1 (the lowest).
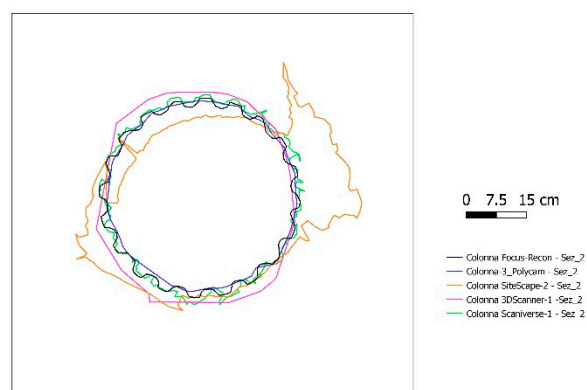
Figure 19. Section 2.
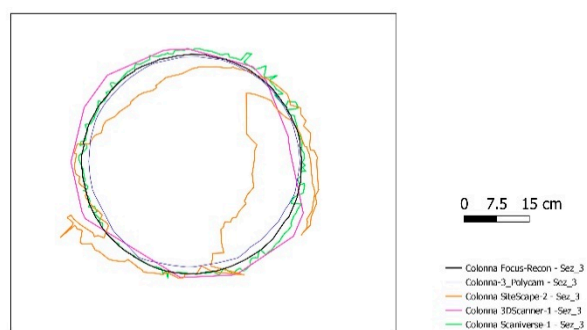
Figure 20. Section 3.
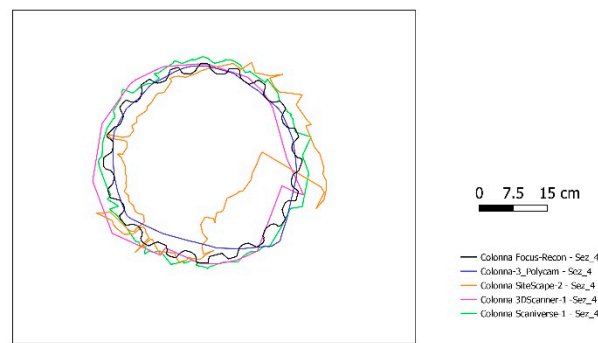
Figure 21. Section 4 (the highest).

From the analysis of these horizontal sections, the poor performances we obtained with Sitescape are, once more, very clear: Sitescape's sections are generally far from the column reconstructed by the TLS (used as ground truth), and are often merely a reconstruction of the column's envelope (see Figure 22). The problems do not depend on the difficulties in the acquisition of the upper sections; they are, indeed, present all over the column height. With regards the other apps, those performing better are certainly Polycam (although it did not correctly retrieve the grooves of the column) and Scaninverse. 3D Scanner is characterized by mixed performances, showing localized discrepancies.

Figure 22. Detail of the Sitescape point cloud.

3.3. Case 3: Facade

The third case consists of a survey of a building facade. The survey using the LiDAR sensor was performed with the iPad screen always parallel to the facade. Likewise in this case, the parameters used were the same as in paragraph 3.1 (Case 1). The validation of the point clouds was performed against data from the TLS Faro Focus 3D acquisition. A single scan was made at $\frac{1}{4}$ resolution, $3\times$ quality (7 mm/10 m resolution) and with an overlap between scans of at least 30%. Acquisition times were relatively short for all four apps: around 1 min. In this respect, the acquisition with the TLS took 6 min for a 360° color scan. Table 8 shows the number of points in the point clouds for the same portion of the wall (Figure 23) for each of the apps and the TLS.

Table 8. Number of points of the point clouds for the facade.

Dataset	N° of Points
Focus 3D	2638.166
Polycam	1145.667
Sitescape	8161.379
3D Scanner App	2941.878
Scaninverse	244.293
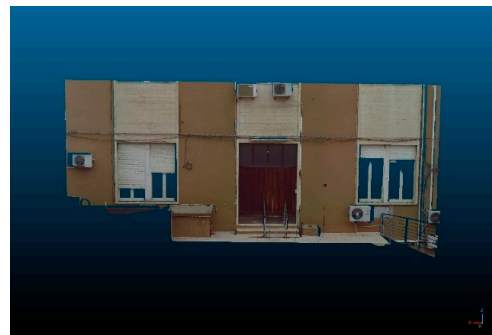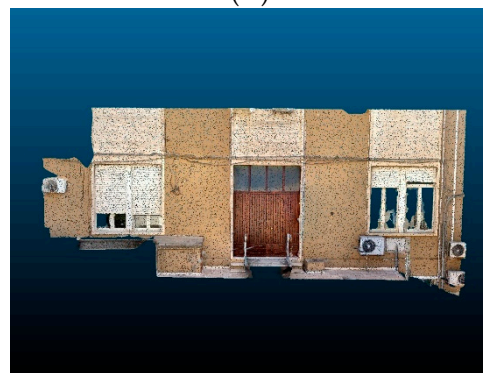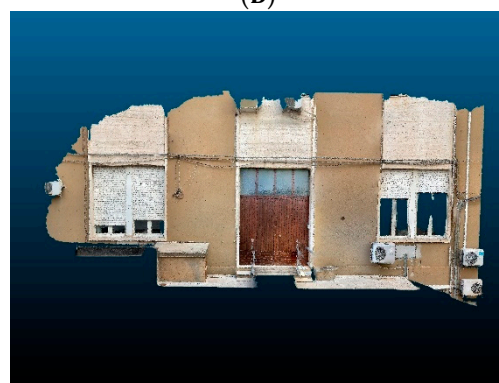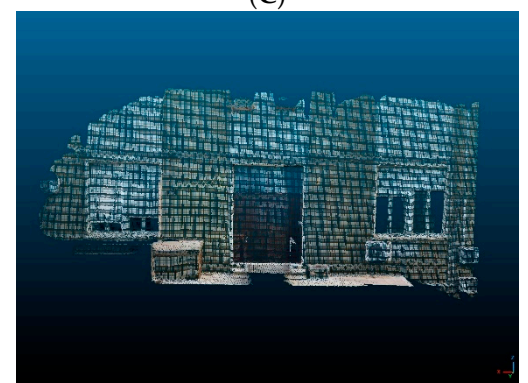
Figure 23. Facade point clouds: (**A**) Focus 3D; (**B**) Polycam; (**C**) Sitescape; (**D**) 3D Scanner; (**E**) Scaninverse.

From Table 8 and Figure 23, the different result qualities are noticeable; in particular, the point cloud obtained using Scaninverse has the lowest resolution, but also Sitescape and 3D Scanner show some problems in obtaining uniform and complete clouds. In addition, for Case 3, the different point clouds have been C2C-compared against the TLS measurements. The comparison results are reported in Tables 9 and 10. As in the two previous cases, the threshold to prevent biases from possible outliers was set at 10 cm consistently: (i) 6% of

the detected points exceeded this threshold for the Polycam, (ii) 5% for Sitescape; (iii) 8% for 3D Scanner; and (iv) 6% for Scaninverse.

Table 9. Statistical parameters of the comparisons between the TLS data and the apps' point clouds.

App	Polycam	SiteScape	3D Scanner	Scaninverse
Min (m)	0	0	0	0
Max (m)	1.084	1.085	0.829	0.791
Mean (m)	0.019	0.024	0.033	0.023
Dev. Stand (m)	0.070	0.066	0.071	0.065

Table 10. C2C analysis—percentages of points in the different distance range.

App	Polycam	SiteScape	3D Scanner	Scaninverse
<1 cm	58%	29%	21%	26%
1 cm–3 cm	24%	41%	35%	48%
3 cm–5 cm	6%	17%	22%	14%
5 cm–10 cm	6%	8%	14%	6%
>10 cm	6%	5%	8%	6%

From Tables 9 and 10 and from Figures 24–27 (showing the discrepancy maps), it is clear that satisfactory results can be obtained with Polycam (which is characterized by a standard deviation of 7 cm and 82% of mismatch between 0 cm and 3 cm). Sitescape and Scaninverse perform similarly and appear to be just slightly worse than Polycam. As for Case 1, 3D Scanner is the app with the lowest accuracy.
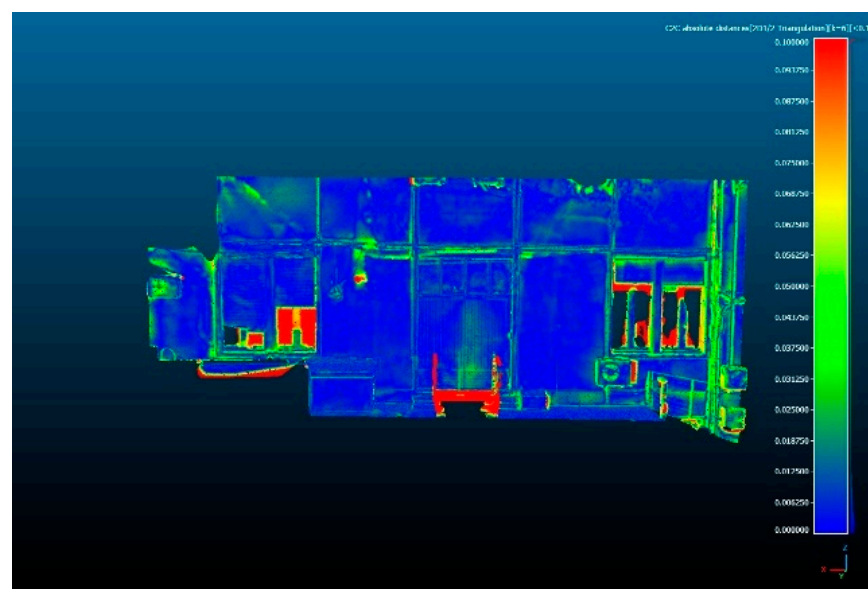
Figure 24. Discrepancy (m) map between TLS' and Polycam's point clouds.
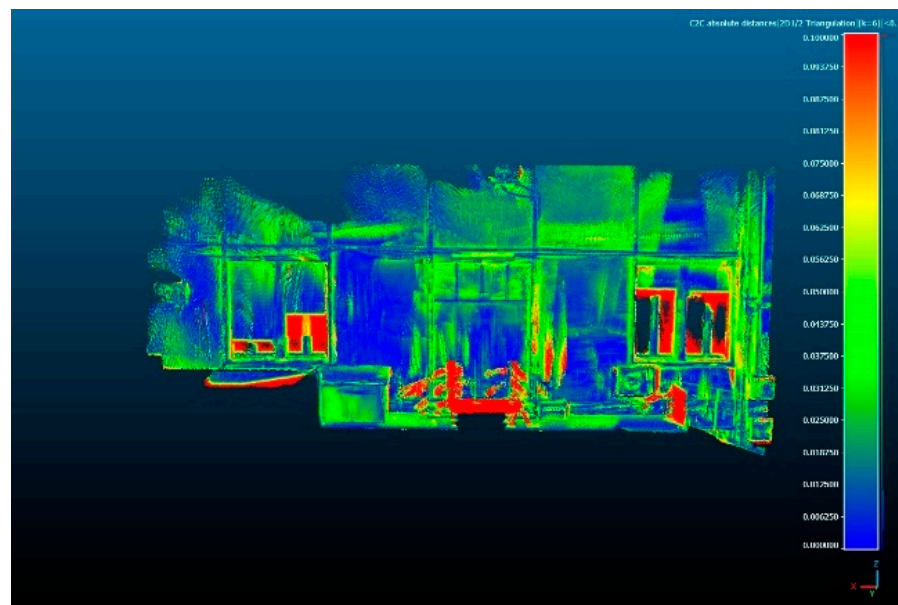
Figure 25. Discrepancy (m) map between TLS' and Sitescape's point clouds.
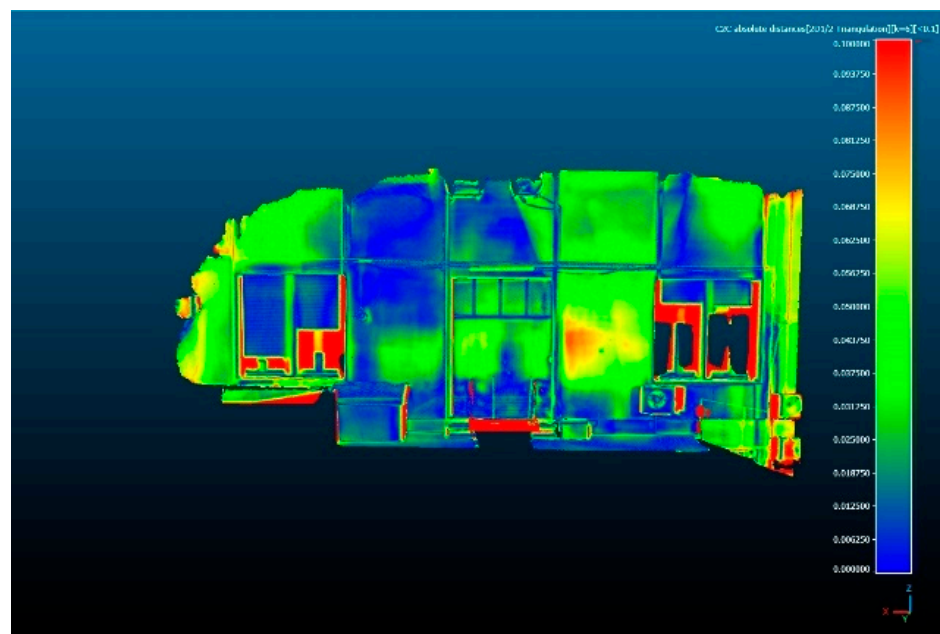
Figure 26. Discrepancy (m) map between TLS' and 3D Scanner's point clouds.
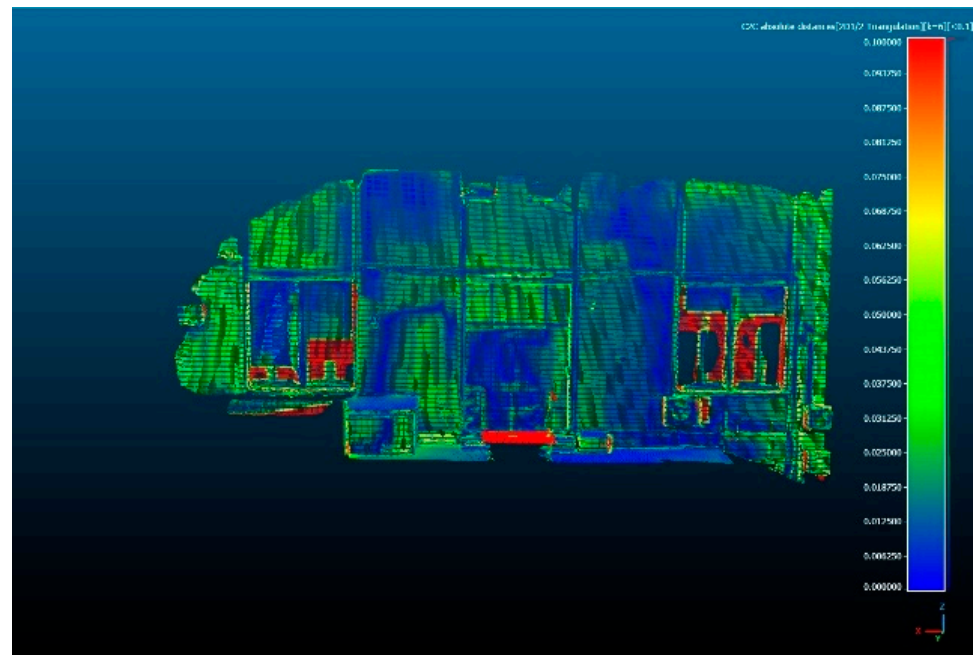
Figure 27. Discrepancy (m) map between TLS' and Scaninverse's point clouds.

3.4. Case 4: Fountain in the Botanical Garden

The fourth case study is a small fountain located in the Botanical Garden of Cagliari.

The survey using the Apple LiDAR sensor was performed at less than 1 m by walking around the fountain. The survey using the HDS7000 TLS was performed in "High" mode, with a resolution of 6.3 mm/10 m. Acquisition times were relatively short for all four apps: around 1 min, whereas 5 min were required for the TLS survey.

Table 11 shows the number of points of the point cloud of the same portion of the fountain (Figure 28).

Table 11. Number of points of the point clouds for the fountain.

Dataset	N° of Points
HDS	898.939
Polycam	237.075
Sitescape	3428.060
3D Scanner App	21.169
Scaninverse	472.280

From the analysis of Table 11 and Figure 28, the 3D Scanner's result seems to have the lowest resolution, whereas Sitescape continues to present the highest number of points acquired.

In this case (Case 4), the results of the C2C-comparison of the measurements provided by each of the four apps and the TLS are summarized in Tables 12 and 13.

From Tables 12 and 13 and from Figures 29–32 (the discrepancy maps), it is clear that all apps are capable of effectively reconstructing the target (standard deviation of about 1 cm and 90% of points with a misfit between 0 cm and 3 cm) when compared to the TLS.
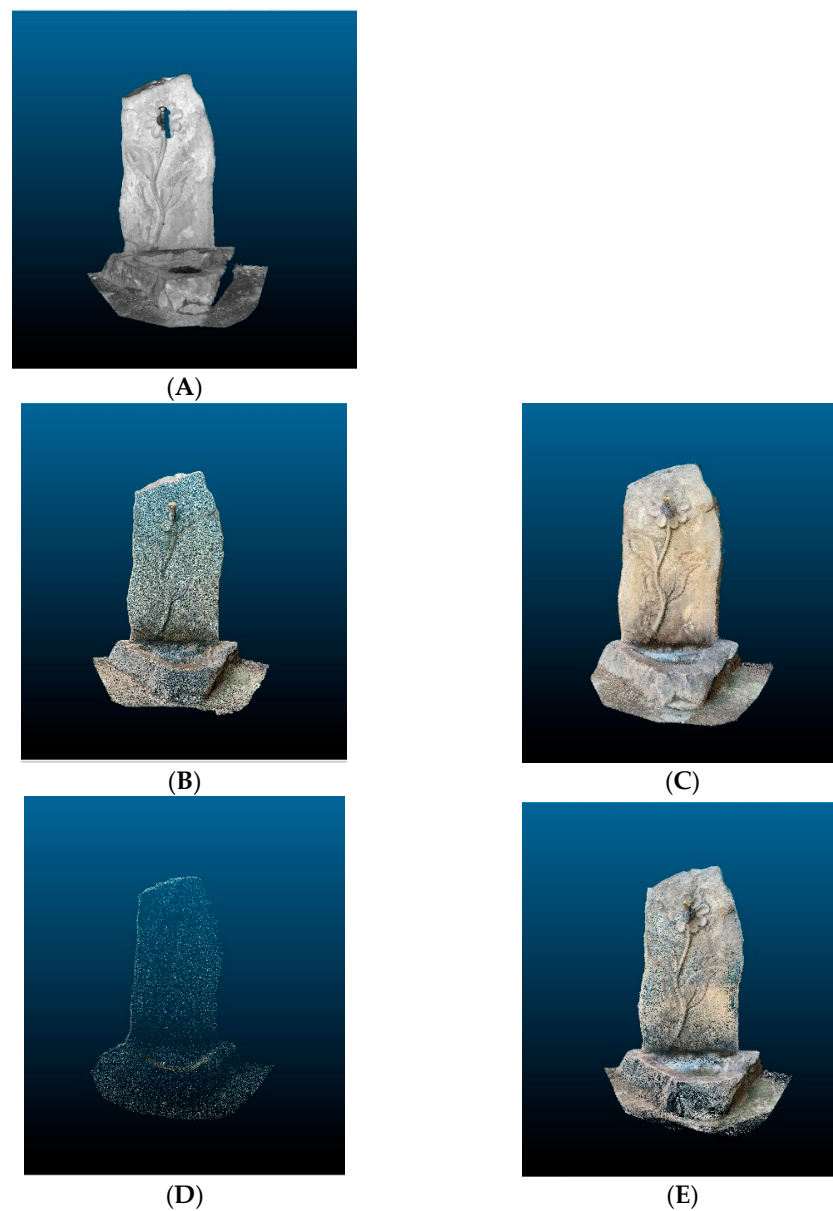
Figure 28. Point clouds of the fountain: (**A**) HDS7000; (**B**) Polycam; (**C**) Sitescape; (**D**) 3D Scanner; (**E**) Scaninverse.

Table 12. Statistical parameters of the comparisons between the TLS data and the apps' point clouds.

App	Polycam	SiteScape	3D Scanner	Scaninverse
Min (m)	0	0	0	0
Max (m)	0.088	0.099	0.081	0.088
Mean (m)	0.006	0.008	0.009	0.003
Dev. Stand (m)	0.013	0.010	0.013	0.004

Table 13. C2C analysis—percentages of points in the different distance ranges.

App	Polycam	SiteScape	3D Scanner	Scaninverse
<1 cm	81%	64%	68%	92%
1 cm–3 cm	13%	32%	24%	5%
3 cm–5 cm	4%	2%	6%	2%
5 cm–10 cm	2%	2%	2%	1%
>10 cm	0%	0%	0%	0%
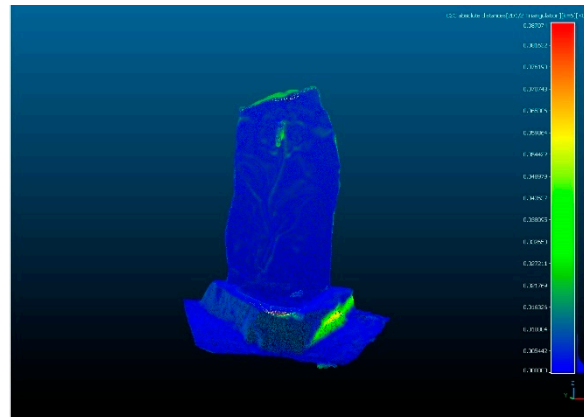
Figure 29. Discrepancy (m) map between TLS' and Polycam's point clouds.
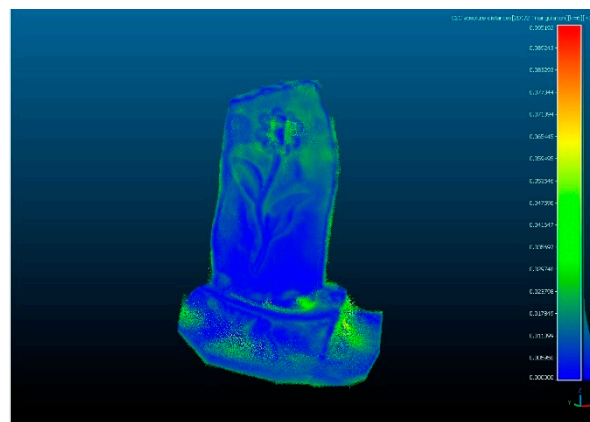
Figure 30. Discrepancy (m) map between TLS' and Sitescape's point clouds.
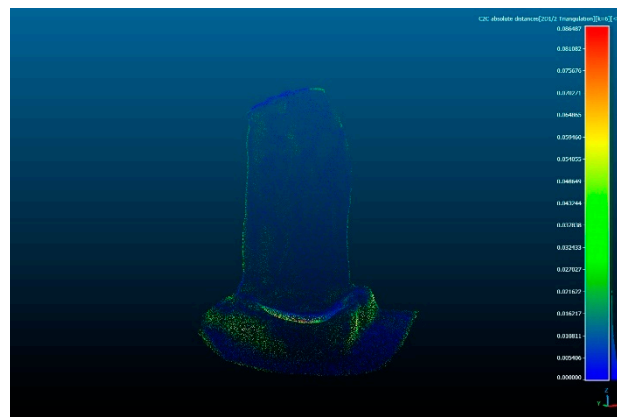
Figure 31. Discrepancy (m) map between TLS' and 3D Scanner's point clouds.
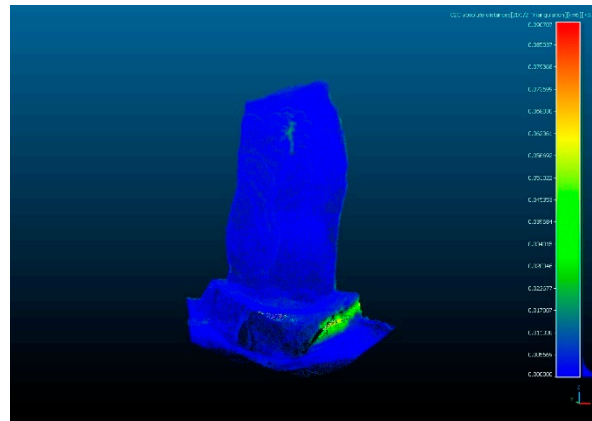
Figure 32. Discrepancy (m) map between TLS' and Scaninverse's point clouds.

3.5. Case 5: Violin

The last case is about a small object: the external case of a violin. The digital reconstruction of the details of such artifacts is crucial to the trackability and optimization of the interventions and work of luthiers. In this specific case, the investigated violin was made in 1793 by the luthiers Giuseppe and Antonio Gagliano.

The LiDAR surveys were performed by moving around the violin case from a distance of 1 m. The used parameters were as follows:

- Polycam: the scan was performed in "Object" mode
- Sitescape: "Point Density" and "Point Size" were set to "High"
- 3D Scanner: the data were acquired in "LiDAR Advanced" mode, selecting "Max Depth" equal to 2 m, "Resolution" equal to 5 mm, "Confidence" equal to "High" and "Masking" equal to "object".
- Scaninverse: the acquisition was conducted in "Small object" mode and processing in "Detail" mode.

Sitescape and 3D Scanner failed in reconstructing the object correctly and, therefore, the corresponding clouds are not considered in the further assessment of Case 5.

Similarly in this case, the violin was surveyed by using a TLS Faro Focus 3D. The scans were performed at a resolution of 1/4, 3× quality (resolution of 7 mm/10 m) and an overlap between the scans of at least 30%. With these parameters, four scans were performed, aligned and processed using the JRC Reconstructor.

From the analysis of Table 14 and from the images of the point clouds (Figure 33), we can draw the preliminary conclusion that the best point cloud is generated by Scaninverse (having the largest number of points and the highest resolution). Also in this case, as ground truth, the apps' clouds have been C2C-compared against the TLS counterparts. Differently from the other cases, for the violin survey the threshold to avoid the detrimental effects of possible outliers was set to 3 cm, and, despite this relatively small distance, no points were discarded (for any of the apps).

Table 14. Number of points of the point clouds for the violin.

Dataset	N° of Points
Focus 3D	81.795
Polycam	118.828
Scaninverse	275.054
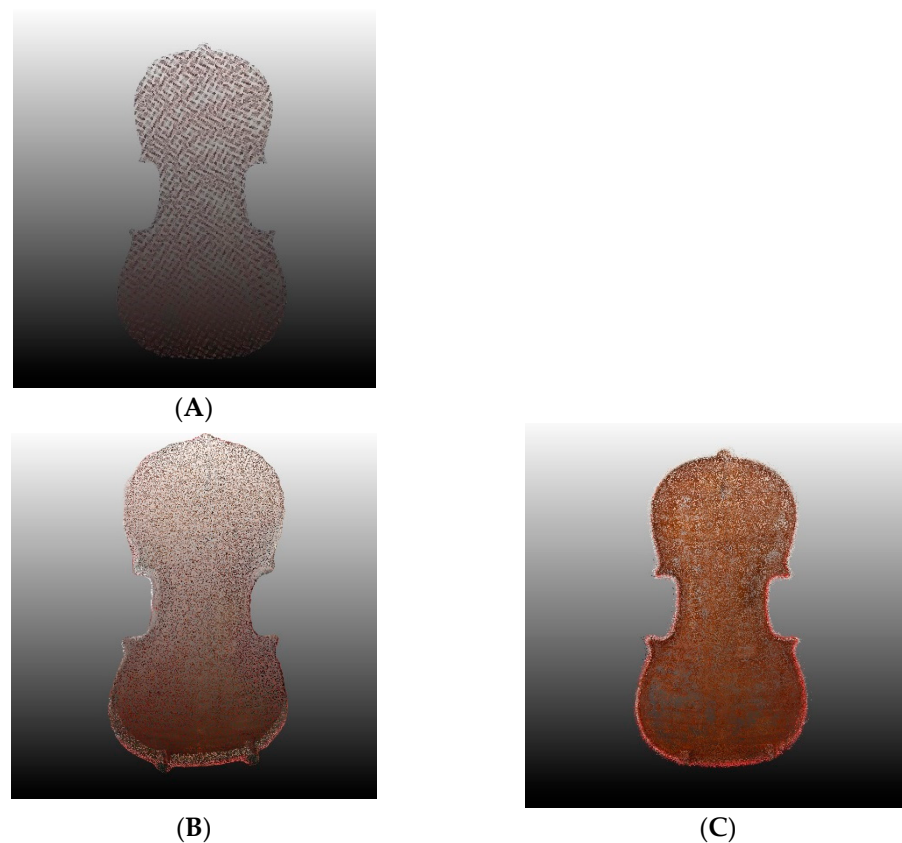
Figure 33. Point clouds of the violin: (**A**) Focus 3D; (**B**) Polycam; (**C**) Scaninverse.

From Tables 15 and 16 and from Figures 34 and 35 (showing the discrepancy maps), both apps provide satisfactory results.

Table 15. Statistical parameters of the comparisons between the TLS data and the apps' point clouds.

App	Polycam	Scaninverse
Min (m)	0	0
Max (m)	0.020	0.012
Mean (m)	0.005	0.001
Dev. Stand (m)	0.001	0.001

Table 16. C2C analysis—percentages of points in the different distance ranges.

App	Polycam	Scaninverse
<1 cm	83%	100%
1 cm–3 cm	17%	0%
3 cm–5 cm	0%	0%
5 cm–10 cm	0%	0%
>10 cm	0%	0%
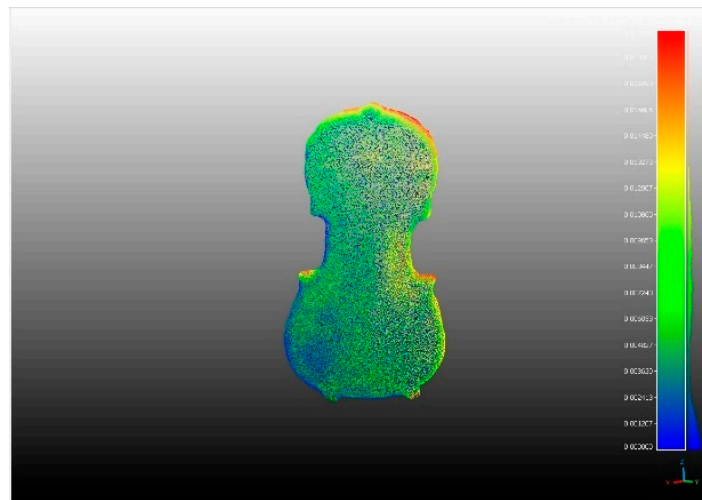
Figure 34. Discrepancy (m) map between TLS' and Polycam's point clouds.
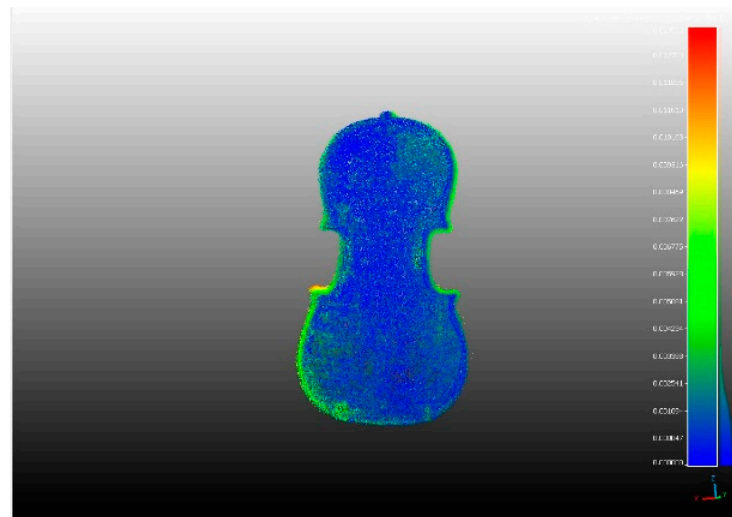
Figure 35. Discrepancy (m) map between TLS' and Scaninverse's point clouds.

4. Discussion

We investigated the Lidar sensor incorporated into the latest generation of Apple iPad, together with four apps specifically developed for the data acquisition and processing of 3D models via that sensor.

The functionality and performance of the LiDAR sensor and of the apps were tested on five different cases of historical, cultural and architectural heritage assets, chosen for being among the most relevant ones for the production of metric documentation. The investigated cases were a cross vault (frequently present in Romanesque and Gothic architecture), a column, a facade of a building, a small fountain and an element of a violin. For all five tests, the functionality, acquisition times, point cloud resolution and 3D model accuracy for each of the four apps were assessed.

With respect to functionality, all four apps present simple and intuitive acquisition settings with the possibility of varying the parameters in relation to the size of the target. In terms of acquisition times, all apps have similar (fast) performances. The most significant difficulty during the acquisitions was estimating the position of the iPad. In particular, in the column's case (Case 2), the Sitescape app was the most affected by this specific problem, resulting in a reconstruction not usable for metric documentation purposes. Concerning the violin case (Case 5), it was impossible to obtain any useful results by using two of the four apps (namely, Sitescape and 3D Scanner). The reason could be the geometric shape of

the element and the too uniform texture; with respect to the texture characteristics of the target, however, previous research applying the same sensor and apps have shown and discussed better results [11].

From these results, we dare to assert that, in line with other research, Apple LiDAR sensors can be a valuable tool for the 3D model creation of architectural and cultural heritage, providing the possibility to contribute to the metric documentation required in the process of knowledge of the asset. However, it is necessary to pay particular attention to certain types of architectural elements that could lead to a result that is not perfectly consistent with reality; see, for example, the column or the violin, which have particular textures or shapes.

5. Conclusions

LiDAR sensors incorporated in prosumers' devices are gaining popularity, especially when considered together with the low-cost software counterparts necessary for effectively handling and processing the data. In this respect, with a limited cost, the user can obtain satisfactory 3D reconstructions of building features and reasonably small artifacts.

These new devices and the associated opportunities pave the way for metric documentation that can be crucial, for example, in facilitating more and more frequent application of HBIM (Historical Building Information Modeling) approaches.

The present work aims at providing a quantitative assessment of some of the most commonly used apps and LiDAR devices, highlighting their potential and possible limitations. As expected, different apps performed better on different application scenarios; however, with the chosen settings, Polycam seems to provide consistently reasonable reconstructions in all the tested cases.

Funding: This research was funded by Fondazione di Sardegna through the grant for "Surveying, modelling, monitoring and rehabilitation of masonry vaults and domes", i.e., Rilievo, modellazione, monitoraggio e risanamento di volte e cupole in muratura (RMMR) (CUP code: F72F20000320007).

Data Availability Statement: Not applicable.

Conflicts of Interest: The author declares no conflict of interest.

References

1. Barsanti, S.G.; Remondino, F.; Fenández-Palacios, B.J.; Visintini, D. Critical factors and guidelines for 3D surveying and modelling in Cultural Heritage. *Int. J. Herit. Digit. Era* **2014**, *3*, 141–158. [CrossRef]
2. Munumer, E.; Lerma, J.L. Fusion of 3D data from different image-based and range-based sources for efficient heritage recording. *Digit. Herit.* **2015**, *304*, 83–86.
3. Deidda, M.; Musa, C.; Vacca, G. A GIS of Sardinia's coastal defense system (XVI–XVIII Century). *Int. Arch. Photogramm. Remote Sens. Spat. Inf. Sci.* **2015**, *XL-4/W7*, 17–22. [CrossRef]
4. Giannattasio, C.; Grillo, S.M.; Vacca, G. Interdisciplinary study for knowledge and dating of the San Francesco convent in Stampace, Cagliari–Italy (XIII-XXI Century). *ISPRS Ann. Photogramm. Remote Sens. Spat. Inf. Sci.* **2013**, *II-5/W1*, 139–144. [CrossRef]
5. Nocerino, E.; Lago, F.; Morabito, D.; Remondino, F.; Porzi, L.; Poiesi, F.; Rota Bulo, S.; Chippendale, P.; Locher, A.; Havlena, M.; et al. A smartphone-based 3D pipeline for the creative industry–the replicate EU project. *Int. Arch. Photogramm. Remote Sens. Spat. Inf. Sci.* **2017**, *XLII-2/W3*, 535–541. [CrossRef]
6. Vacca, G. UAV Photogrammetry for Volume Calculations. A Case Study of an Open Sand Quarry. In *Computational Science and Its Applications–ICCSA 2022 Workshops*; ICCSA 2022, Lecture Notes in Computer Science; Gervasi, O., Murgante, B., Misra, S., Rocha, A.M.A.C., Garau, C., Eds.; Springer: Cham, Germany, 2022; Volume 13382. [CrossRef]
7. Brandolini, F.; Patrucco, G. Structure-from-Motion (SFM) Photogrammetry as a Non-Invasive Methodology to Digitalize Historical Documents: A Highly Flexible and Low-Cost Approach? *Heritage* **2019**, *2*, 2124–2136. [CrossRef]
8. Parrinello, S.; Dell'Amico, A. Experience of Documentation for the Accessibility of Widespread Cultural Heritage. *Heritage* **2019**, *2*, 1032–1044. [CrossRef]
9. Janiszewski, M.; Torkan, M.; Uotinen, L.; Rinne, M. Rapid Photogrammetry with a 360-Degree Camera for Tunnel Mapping. *Remote Sens.* **2022**, *14*, 5494. [CrossRef]
10. Teppati Losè, L.; Chiabrando, F.; Giulio Tonolo, F. Documentation of Complex Environments Using 360° Cameras. The Santa Marta Belltower in Montanaro. *Remote Sens.* **2021**, *13*, 3633. [CrossRef]

11. Vacca, G.; Dessi, A. Geomatics Supporting Knowledge of Cultural Heritage Aimed at Recovery and Restoration. *Int. Arch. Photogramm. Remote Sens. Spat. Inf. Sci.* **2022**, *43*, 909–915. [CrossRef]

12. Grillo, S.M.; Pilia, E.; Vacca, G. Integrated study of the Beata Vergine Assunta dome with Structure from Motion and diagnostic approaches. *Int. Arch. Photogramm. Remote Sens. Spat. Inf. Sci.* **2019**, *XLII-2/W11*, 579–585. [CrossRef]

13. Aita, D.; Barsotti, R.; Bennati, S.; Caroti, G.; Piemonte, A. 3-Dimensional geometric survey and structural modelling of the dome of Pisa cathedral. *Int. Arch. Photogramm. Remote Sens. Spat. Inf. Sci.* **2017**, *XLII-2/W3*, 39–46. [CrossRef]

14. Park, G.; Lee, J.H.; Yoon, H. Semantic Structure from Motion for Railroad Bridges Using Deep Learning. *Appl. Sci.* **2021**, *11*, 4332. [CrossRef]

15. Mandirola, M.; Casarotti, C.; Peloso, S.; Lanese, I.; Brunesi, E.; Senaldi, I. Use of UAS for damage inspection and assessment of bridge infrastructures. *Int. J. Disaster Risk Reduct.* **2022**, *72*, 102824. [CrossRef]

16. Garcia Millan, V.E.; Rankine, C.; Sanchez-Azofeifa, G.A. Crop Loss Evaluation Using Digital Surface Models from Unmanned Aerial Vehicles Data. *Remote Sens.* **2020**, *12*, 981. [CrossRef]

17. Hasheminasab, S.M.; Zhou, T.; Habib, A. GNSS/INS-Assisted Structure from Motion Strategies for UAV-Based Imagery over Mechanized Agricultural Fields. *Remote Sens.* **2020**, *12*, 351. [CrossRef]

18. Grottoli, E.; Biausque, M.; Rogers, D.; Jackson, D.W.T.; Cooper, J.A.G. Structure-from-Motion-Derived Digital Surface Models from Historical Aerial Photographs: A New 3D Application for Coastal Dune Monitoring. *Remote Sens.* **2021**, *13*, 95. [CrossRef]

19. De Marco, J.; Maset, E.; Cucchiaro, S.; Beinat, A.; Cazorzi, F. Assessing Repeatability and Reproducibility of Structurefrom-Motion Photogrammetry for 3D Terrain Mapping of Riverbeds. *Remote Sens.* **2021**, *13*, 2572. [CrossRef]

20. García-Gómez, P.; Royo, S.; Rodrigo, N.; Casas, J.R. Geometric model and calibration method for a solid-state LiDAR. *Sensors* **2020**, *20*, 2898. [CrossRef]

21. Wang, D.; Watkins, C.; Xie, H. MEMS mirrors for LiDAR: A review. *Micromachines* **2020**, *11*, 456. [CrossRef]

22. Aijazi, A.K.; Malaterre, L.; Trassoudaine, L.; Checchin, P. Systematic evaluation and characterization of 3d solid state lidar sensors for autonomous ground vehicles. *Int. Arch. Photogramm. Remote Sens. Spat. Inf. Sci.* **2020**, *XLIII-B1-2020*, 199–203. [CrossRef]

23. Murtiyoso, A.; Grussenmeyer, P.; Landes, T.; Macher, H. First assessments into the use of commercial-grade solid state lidar for low cost heritage documentation. *Int. Arch. Photogramm. Remote Sens. Spat. Inf. Sci.* **2021**, *XLIII-B2-2*, 599–604. [CrossRef]

24. Gollob, C.; Ritter, T.; Kraßnitzer, R.; Tockner, A.; Nothdurft, A. Measurement of Forest Inventory Parameters with Apple iPad Pro and Integrated LiDAR Technology. *Remote Sens.* **2021**, *13*, 3129. [CrossRef]

25. Tontini, A.; Gasparini, L.; Perenzoni, M. Numerical model of spad-based direct time-of-flight flash lidar CMOS image sensors. *Sensors* **2020**, *20*, 5203. [CrossRef] [PubMed]

26. Luetzenburg, G.; Kroon, A.; Bjørk, A.A. Evaluation of the Apple iPhone 12 Pro LiDAR for an Application in Geosciences. *Sci. Rep.* **2021**, *11*, 22221. [CrossRef] [PubMed]

27. Teppati Losè, L.; Spreafico, A.; Chiabrando, F.; Giulio Tonolo, F. Apple LiDAR Sensor for 3D Surveying: Tests and Results in the Cultural Heritage Domain. *Remote Sens.* **2022**, *14*, 4157. [CrossRef]

28. Díaz-Vilariño, L.; Tran, H.; Frías, E.; Balado, J.; Khoshelham, K. 3D mapping of indoor and outdoor environments using Apple smart devices. *Int. Arch. Photogramm. Remote Sens. Spat. Inf. Sci.* **2022**, *XLIII-B4-2022*, 303–308. [CrossRef]

29. iPad Pro-Apple. Available online: https://www.apple.com/ipad-pro/ (accessed on 5 October 2022).

30. PolyCam. Available online: https://poly.cam/ (accessed on 5 October 2022).

31. SiteScape. Available online: https://www.sitescape.ai/ (accessed on 5 October 2022).

32. 3d Scanner App. Available online: https://3dscannerapp.com/ (accessed on 5 October 2022).

33. Scaninverse. Available online: https://scaniverse.com/ (accessed on 5 October 2022).

34. Reconstructor Software. Available online: https://gexcel.it/it/software/reconstructor (accessed on 5 October 2022).

35. CloudCompare Software. Available online: https://www.cloudcompare.org/main.html (accessed on 10 October 2022).

36. Grillanda, N.; Chiozzi, A.; Bondi, F.; Tralli, A.; Manconi, F.; Stochino, F.; Cazzani, A. Numerical insights on the structural assessment of historical masonry stellar vaults: The case of Santa Maria del Monte in Cagliari. *Contin. Mech. Thermodyn.* **2021**, *33*, 1–24. [CrossRef]